Freie Universität Berlin - Department of Earth Sciences
Planetary Geodynamics Group

DOCUMENTATION

Rocky and Ocean Worlds' Structure (ROWS) model

Documentation author:
Iris Boer

Code author:
Lena Noack

August 25, 2025

Contents

1 Introduction

The Rocky and Ocean Worlds' Structure (ROWS) model is a one-dimensional Python code written by Prof. Dr. Lena Noack for educational purposes. Its primary purpose is to provide an accessible yet scientifically grounded framework for modeling the internal structure of rocky planetary bodies. Based on a small set of user-defined parameters, including the planetary mass and iron content, this code enables first-order estimations of planetary radius and the internal distribution of key physical properties. These physical properties include depth-dependent profiles of key density, pressure, temperature and more. Hence, variation of input parameters allows for users to investigate how these parameters affect the internal structure of a planet, besides the planetary radius.

Code functionality. The code computes radial profiles of several depth-dependent physical properties, including: density, pressure, gravity, temperature, thermal expansion coefficient, heat capacity, mass, electrical conductivity, seismic velocities, bulk and shear modulus. The model assumes spherical symmetry and hydrostatic equilibrium. The internal structure is computed by solving the relevant Equations of State using user-defined bulk parameters. Based on the total mass, iron and water content, the code determines whether and how the planet is differentiated into a metallic core, silicate mantle, liquid water or high pressure ice layer. Additional options allow for further customization of the modeled planet, including primarily, but not limited to, the customization of core composition with the option to add lighter elements and other initial parameters like crust and lithosphere thickness.

Intended Use and Learning Outcomes. The code is suited for scenarios where transparent, foundational models models are appropriate, such as educational settings, as well as research studies, whereas the code shows sufficient amount of reliability. It allows users to investigate how internal properties vary with basic planetary characteristics, and how assumptions about composition influence key outputs like planetary radius and thermal structure. By enabling controlled variation of input parameters, the code supports the understanding of the physical principles governing planetary interiors. It also illustrates the impact of modeling assumptions, highlighting uncertainties that arise from choices like equation-of-state parameters, layer compositions, or elemental content. This manual serves both as a user guide and a conceptual introduction to the principles of interior structure modeling. Aiming to make the code accessible to a range of users, including students (even those with limited programming experience), researchers, and scientifically curious users. The manual combines practical instructions with theoretical background, guiding users through the code's setup, execution, and output interpretation. Its goal is to provide a clear, step-by-step learning path for understanding and effectively using the ROWS model within the context of planetary science.

This ROWS model is based on and builds upon the foundational work from Noack et al. [2016].

2 Running the code

2.1 Initial setup

- Download the ROWS model ZIP file (Link to code). The folder includes 5 files:
  - `Interior_Structure.ipynb`: Main routine.
  - `values.py`: Python script including species characteristics (EOS properties).
  - `EOS_functions.py`: Python script including Equations of State functions to calculate thermodynamic properties.
  - `Help_functions.py`: Python script including functions that calculate melting and sublimation curves.
  - `water.py`: Python script including Equations of State function specifically to calculate thermodynamic properties of water.
- Extract the file into the desired path.
- Open `Interior_Structure.ipynb` in an IDE software (*Refer to Using an IDE interface*).

2.2 Using an IDE interface

Note: This section of the tutorial can be skipped for more advanced users.

An Integrated Development Environment, short for IDE, is a software application that provides the tools to edit and execute code. Any IDE supporting Python can be used to compile the ROWS code (VS Code, PyCharm, Spyder, Google Colab...). The choice of an IDE depends on one's preference. The following section introduces the interface of an IDE and demonstrates its usage.

- **Setup:** Install the IDE of your choice, preferably from its official website. Follow the installation steps (usually just clicking "Next" a few times).
- **Opening a project:** After opening your installed IDE, select "Open Folder/Project" and enter the path where you stored the `ROWS_Interior-Structure-Model` folder.
- **Running the scripts:** Open the `Interior_Structure.ipynb` notebook where direct changes can be made and the code can be run. Customize the parameters as you want in this file or use the test cases found in Section 3. Once done, you can run the script by just clicking the "Run all" button, usually displayed as a "Play" button. If not found, the following shortcut can be used to run the notebook: *Windows/Linux: Ctrl + F9 and macOS: Cmd + F9.*

2.3 Essential libraries

Libraries are code add-ons that enhance the functionality of code by incorporating several functions. The ROWS code uses standard library modules only. These library modules are already included in Python and therefore do not need to be installed. The ROWS code uses: `numpy`, `math`, `csv`, `pandas`, `matplotlib` and `os`. The libraries are extracted at the beginning of `Interior_Structure.ipynb`:

```
import numpy as np
import math
import csv
import pandas as pd
import matplotlib.pyplot as plt
import os
```

2.4 ROWS Code Workflow

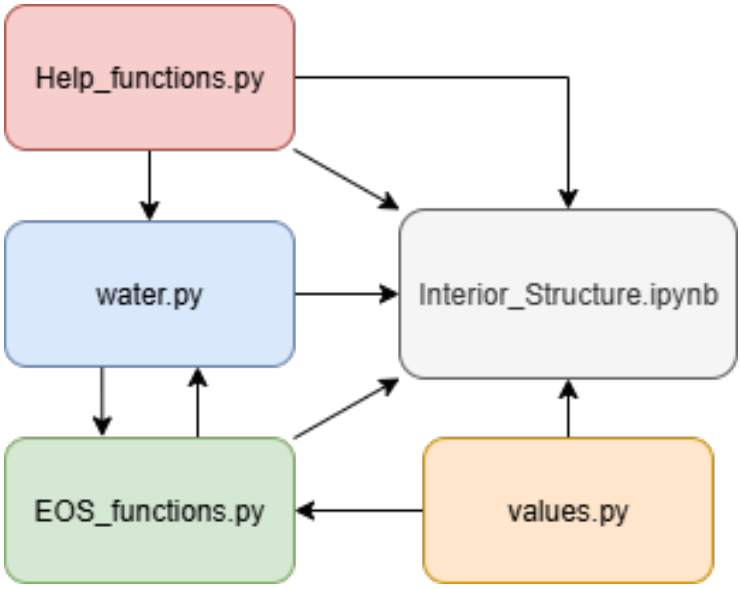

Figure 1: ROWS code workflow. Illustration of the interaction between the scripts.

2.5 Executing the code

Important: Only edit `Interior_Structure.ipynb`. Do not change the other scripts.

- Open `Interior_Structure.ipynb`. Notice the first cells in the script. If you are using *Google Colab*, ensure you connect to your Google Drive by running these cells. Ensure you update the default file directory to match your current working path. If you are using another IDE, these cells can be ignored or removed. In all cases, make sure that the file directory is correct and do not modify any other part of the setup.

- Run the entire notebook. During execution of the notebook, the model automatically is set (via the main function `interior_structure(M,x_Fe_tot,x_H2O_tot)`) to generate and plot the first two benchmarks (see Section 3). This happens under the sections 'Example 1: Earth reproduction' and 'Example 2: Ocean world' in the notebook.

- To run the simulation with custom input parameter values, 'Example 1: Earth reproduction' provides a general setup and allows for easy adaptions of the input parameters. If you wish to change other parameters in the notebook please restart and re-run the entire notebook first. If you do not wish to regenerate the default benchmark data and plots, you can comment out the corresponding section.

- To perform multiple simulations with variation of parameters, go to 'Variation plots' section. This section includes a script for extracting, storing, and visualizing data, along with two blocks for parameter variations. These parameter variations cells can be uncommented and used to explore parameter dependencies. The execution of these cells will generate a 'Data' folder containing data files (`.csv`) with output values from each simulation. These data files are named after the varied parameter and its corresponding value, followed by `_interior_data`. The data files include data for `Rp_E` (planetary radius), `Rc_E` (core radius), `Rm_E` (mantle radius), `MOI` (moment of inertia), `radius` (radial distance), `density` (material density), `gravity` (gravitational acceleration), `pressure` (pressure), `temperature` (temperature), `alpha` (thermal expansion coefficient), `cp` (specific heat capacity), `mass` (mass), `elcond` (electrical conductivity), `vP` (primary wave velocity), `vS` (secondary wave velocity), `KT` (isothermal bulk modulus), `KS` (adiabatic bulk modulus), `mu` (shear modulus), `mat` (material types).

3 Test cases/Benchmarks

Note: Refer to Section 4.1 for a detailed description of the parameters.

3.1 Example 1: Earth reproduction

The first straightforward benchmarking is reproducing Earth's bulks properties. When running the notebook, data that closely approximate Earth's internal profile is being generated and plotted using the following input parameters:

```
M=1, x_Fe_tot=38, x_H2O_tot=0.023
```

The figure that is being produced should be identical to Figure 3. In the shown profiles, colors are used to represent different compositional layers. The legend in Fig. 2 indicates which color corresponds to which composition. The colors are based on material types that are assigned in `mat` array. The resulting internal structure profiles (Figure 3) are in good agreement with empirical Earth models such as PREM (Preliminary Reference Earth Model) [Dziewonski and Anderson, 1981], especially in capturing the general trends in seismic wave measurements. Some differences may arise due to simplified mineralogical assumptions or equation-of-state formulations, but the overall structural features are consistent with expectations. These input parameters yield a total planetary radius of 6378 km and a core radius of approximately 3501 km, as shown in Table 1. According to PREM, the seismically inferred core radius of Earth is about 3480 km, indicating that the model reproduces both quantities with relative good accuracy. Because Earth is the best-studied terrestrial planet, successful reproduction of its interior serves as a robust benchmark for evaluating other model runs and variations.

Figure 2: Legend showing the color scheme used to represent interior layers based on composition. The value behind the compositions indicates their designated value in the `mat` array.

3.2 Example 2: Ocean world

In addition to iron, water content (`x_H2O_tot`) is a critical compositional parameter in determining the structure of planets. Within the ROWS model, the total water budget is specified by the user as a weight percentage. Although water usually constitutes a relatively small fraction of planetary mass in most rocky planets, it can have a strong effect on physical properties, particularly in the outer layers. Unlike iron, water does not partition into the core. It is instead distributed between the mantle and the outermost layers. Depending on the conditions such as pressure and temperature, water will set into the mantle, form high pressure ice or exist as liquid water (ocean). An example for a more water-rich planet is shown in Fig 4. Figure 4 shows an example of a water-rich planet generated by increasing the water content in the Earth-like simulation from Section 3.1 to `x_H2O_tot = 40`. In this case, increasing water content leads to an increase in planetary radius due to the relatively low density of water-bearing minerals and/or the presence of a surface water layer, as shown in Fig 4. Due to water concentrating mainly in the upper-mantle and crust, the impact of water on planetary interior structure is generally confined to the outer regions.

The water content parameter provides potential to investigate and explore different kinds of planetary structures. The planet's mass strongly influences the pressure profile, and so the form water will be present in (e.g., hydrated minerals, high-pressure ice, or liquid ocean). In addition, the potential surface temperature (`T_surf`) can be manually adjusted in the code. For instance, setting `T_surf = 270 K` (below the freezing point of water) while running the parameters used for Fig 4 allows the simulation of a planet with a liquid subsurface ocean sandwiched between two ice layers. In this example, the icy layer is thin, but varying the combination of water content, planetary mass, and surface temperature allows modeling of different types of ocean worlds, showing how water distributes in the outer layers depending on thermal and compositional conditions.

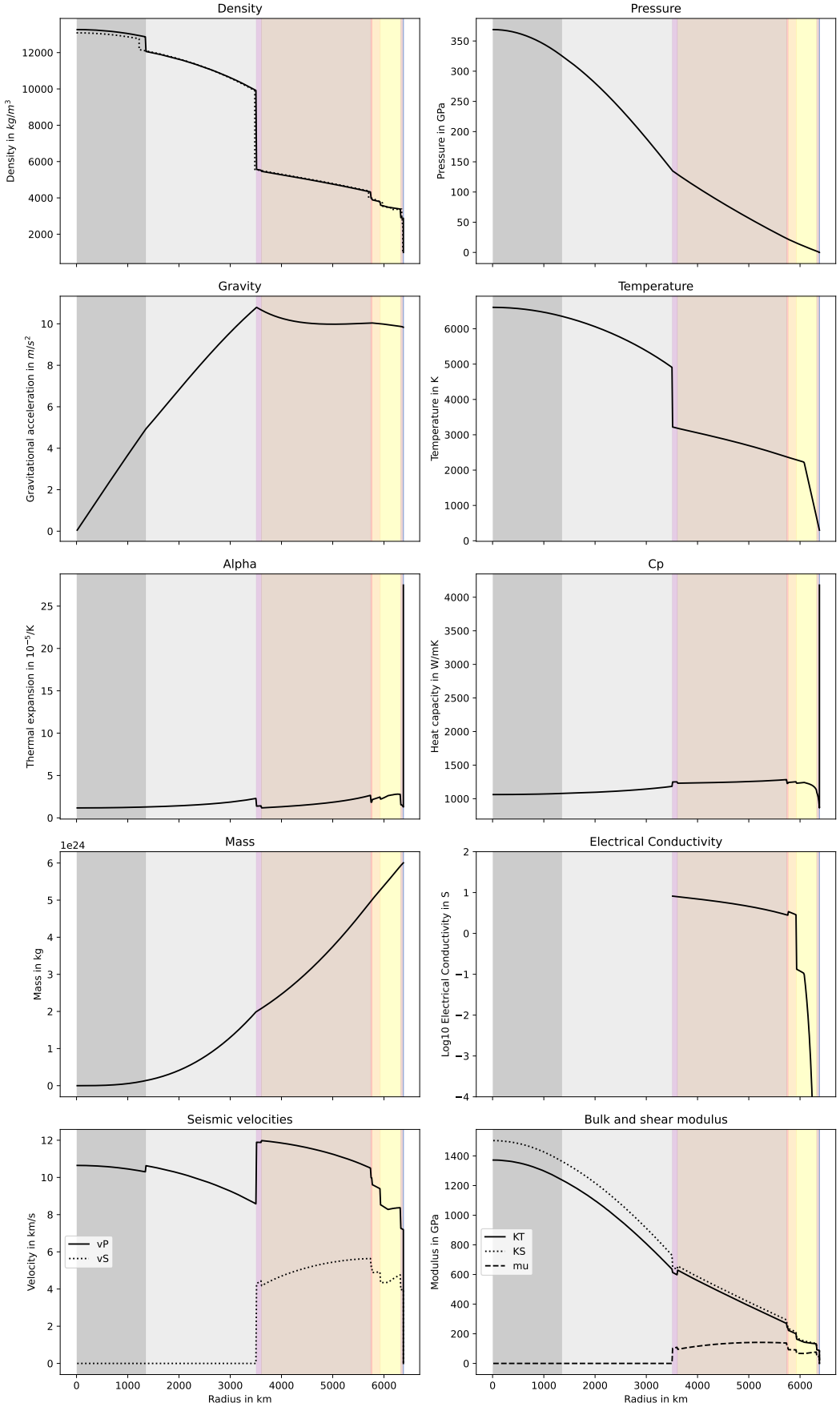

Figure 3: Modeled Earth-like interior profiles for M = 1, x_Fe_tot = 38, x_H2O_tot = 0.023. The density profile includes a dotted line that presents the density profile based on PREM data. See Fig. 2 for the corresponding color legend.

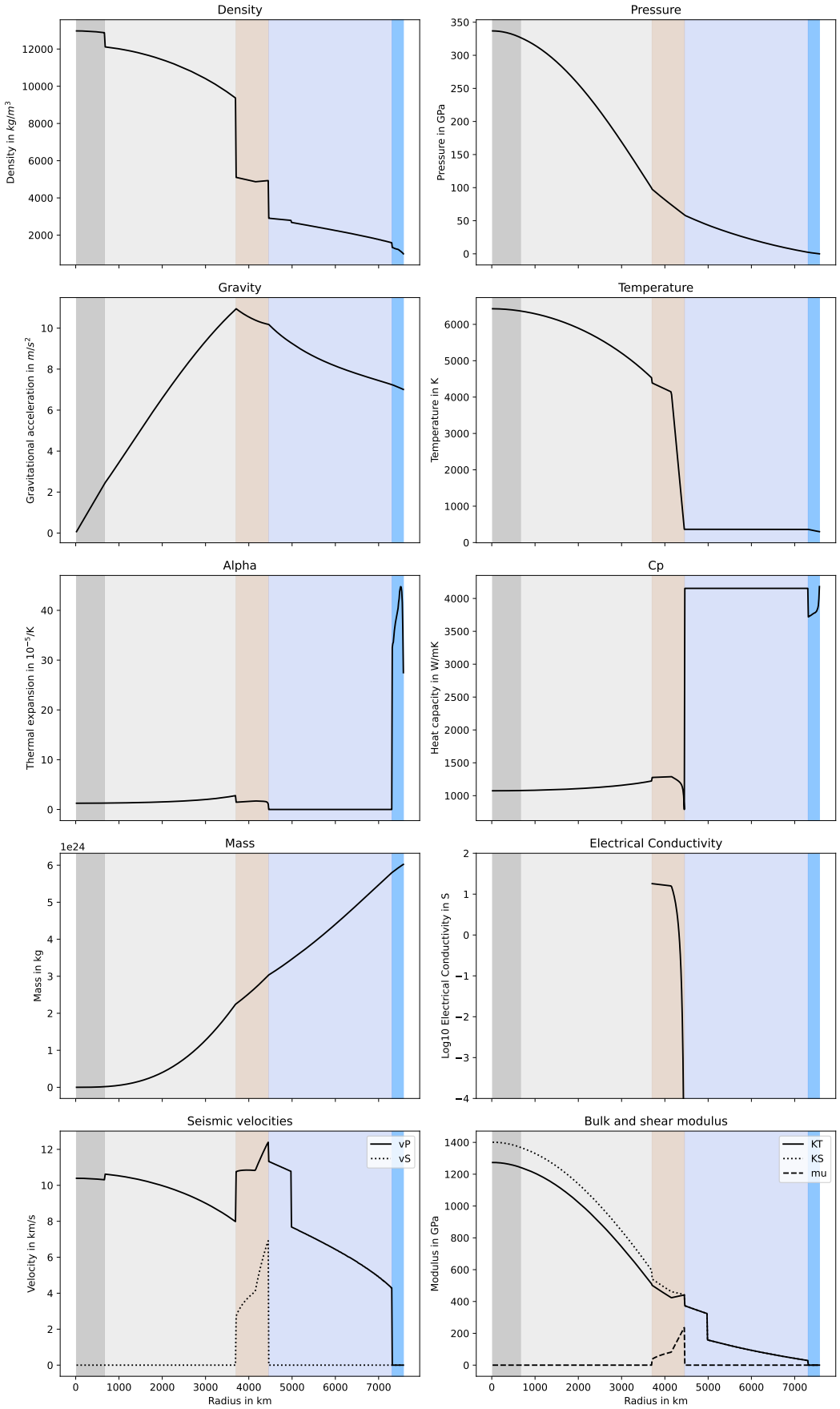

Figure 4: Modeled interior profiles for M = 1, x_Fe_tot = 38, x_H2O_tot = 40. See Fig. 2 for the corresponding color legend.

3.3 Example 3: Fe content variation

Iron content [wt%]	Calculated Radius (R⊕ & km)		Core size (R⊕ & km)	
0	∼1.087	∼6925	No core	No core
5	∼1.076	∼6854	No core	No core
15	∼1.054	∼6713	∼0.346	∼2207
25	∼1.031	∼6571	∼0.458	∼2918
35	∼1.009	∼6427	∼0.531	∼3384
38	**∼1.001**	**∼6378**	**∼0.549**	**∼3501**
45	∼0.985	∼6276	∼0.589	∼3750
55	∼0.960	∼6119	∼0.638	∼4065
65	∼0.935	∼5956	∼0.682	∼4346

Table 1: Effect of iron content variation on estimated planetary radius (for a 1 M⊕ planet). The values that most closely match Earth's are highlighted in bold. For this Earth case the water content was set to `x_H2O_tot = 0.023`, whereas in all other cases `x_H2O_tot = 0` was used.

The iron content (`x_Fe_tot`) of a terrestrial rocky planet is a key compositional parameter that significantly influences its interior structure and bulk radius. Within this interior structure code, the total iron budget of the planet is defined by the user as a weight percentage via the parameter `x_Fe_tot` in the main function call:

```
interior_structure(M, x_Fe_tot, x_H2O_tot)
```

This value can range from 0 to 100 (in weight percent), where 0 would represent an entirely iron-free planet and 100 a purely iron planet. While such extreme values are not necessarily physically plausible, the code is built to handle them for theoretical completeness and robustness.

The planetary iron content governs the size and mass of the planet's core, which is assumed to be composed primarily of iron. As per geophysical and geochemical models of planetary differentiation, the majority of the planet's iron resides in the metallic core due to its high density and siderophile nature. The iron in the core can potentially alloyed with a light element such as silicon (FeSi), carbon (FeC), sulfur (FeS), or oxygen (FeO), which the user can specify. This choice is controlled by the parameter:

```
elem = elem    # Specify light element in the core: Fe, FeSi, FeC, FeS, or FeO
```

This flexibility enables more realistic representations of core chemistry based on different planetary formation scenarios. For more details on this, see Section 3.6. The distribution of iron between the core and mantle is handled internally, ensuring consistency with the user-specified mantle iron number. Most of the iron is directed into the core, but a fixed fraction can remain in the mantle, determined by the mantle's target iron number. If the specified `x_Fe_tot` is insufficient to achieve the target mantle iron number and still allow for a core, the code gives an error message:

```
''Error, not enough iron in planet to have  0.1  as iron number -> adapt iron number!''
```

The minimum to satisfy the mantle iron number depends on other parameters such as the water content. However, even when the set mantle iron number cannot be established, the code will continue by assuming a coreless planet (see Table 1) and reallocates all iron to the mantle. In such cases, the mantle iron number is adjusted accordingly to reflect the actual iron distribution. The iron content has a notable effect on both the mass and radius of the planetary core, as well as the planet's total radius. Higher iron fractions result in denser planets with more massive cores and correspondingly smaller radii due to the compact nature of metallic iron. Table 1 summarizes the effect of varying x_Fe_tot on selected structural parameters. As expected, an increasing iron budget correlates with a decreasing planetary radius and an increasing core mass fraction. To benchmark the code's performance and validate its physical consistency, we investigate the impact of varying the total iron content parameter, `x_Fe_tot`, on key structural properties of terrestrial planets. Like said before, iron plays a central role in planetary differentiation due to its siderophile nature, tending to concentrate in the metallic core. Consequently, increasing the iron fraction leads to denser interior structures, larger core masses, and smaller total planetary radii, reflecting the high density and compactness of metallic iron. Table 1 presents the model outputs across a range of `x_Fe_tot` values, illustrating how changes in iron abundance affect the planet's overall structure. The results show the expected trends: as more iron is available, the mass fraction of the core (which consistent primarily out of iron) increases while the total planetary radius decreases. This confirms the model's ability to reproduce realistic geophysical behavior.

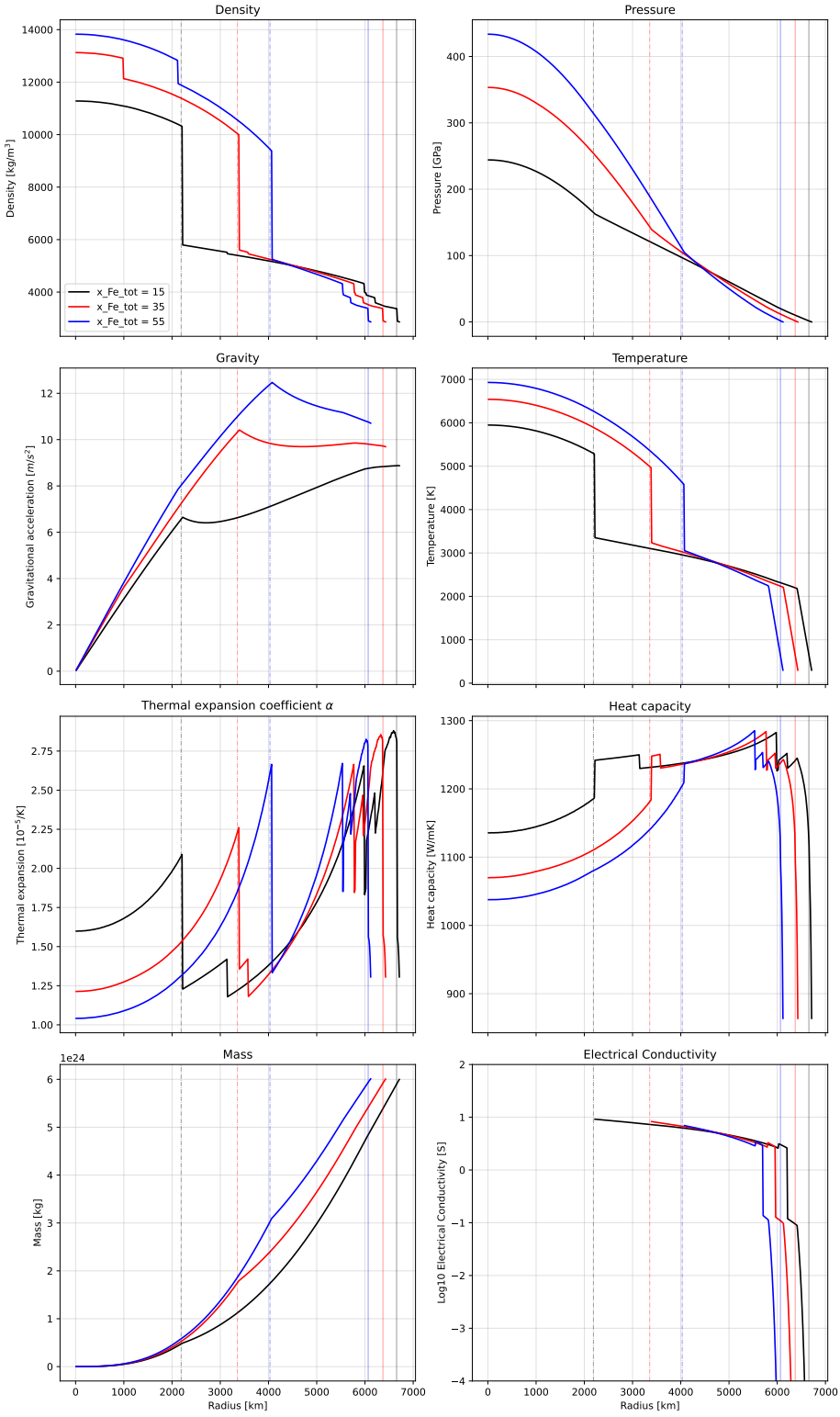

Figure 5: Effect of varying iron content on internal structure profiles. The faint dashed lines indicate the core radius, while the faint solid line represents the mantle radius of planets modeled with different iron contents. All other parameters are held at their default values.

Effect of Iron on Planetary Interior Structure Figure 5 provides a graphical illustration of how varying `x_Fe_tot` alters internal structure properties. As iron abundance increases, the core becomes larger and more massive, compressing the mantle and reducing the overall radius. The effect is non-linear due to complex interactions between core composition, mantle mineralogy, and pressure-density relations. Figure 5 can be reproduced by uncommenting the code under the 'Fe variation data' section in the notebook. Each profile corresponds to a model with different total iron mass fractions: 15% (black), 35% (red), and 55% (blue). The trends across these profiles offer insight into how iron influences planetary structure and composition.

Affect of Core mass fraction As expected, increasing the total iron content leads to significantly higher densities throughout the planetary core. One can see that after the Core-Mantle-Boundary (CMB) density are generally similar again. Similar core-specific behavior is shown for the pressure, gravity and temperature profile: A higher iron content results into larger cores, leading to higher pressure, temperature and gravity acceleration values in the planet's core. The gravitational acceleration increases with iron content due to the higher concentration of mass towards the center, causing this local maximum at the CMB. This is a typical feature and can be used as a benchmark of rocky terrestrial planet that have a metallic core; core-less planets do not have this feature. Higher iron content results in general higher temperatures in the core, due to greater core compression. While surface temperatures are similar, the core's thermal behavior strongly diverges between layers. Furthermore, the thermal expansion coefficient varies significantly with depth and Fe content. Heat capacity exhibits subtle changes with iron content. The more iron-rich the planet, the higher the heat capacity in the deeper regions, driven by the core's metallic composition. The cumulative mass profile confirms that iron-rich planets are more centrally concentrated. For the same total planetary mass, planets with higher iron content have larger cores, which dominate the mass distribution. The electrical conductivity profile is relatively similar for different iron contents as it is calculated only for regions above the CMB and mostly determined by the water content.

Taken together, an increasing iron content should lead to:

- A denser and more compact planet,
- A larger and more massive core,
- Higher interior pressures and temperatures at greater depths (below CMB)
- Shifts in gravity, heat capacity and mass profiles,

These variations underscore the importance of accurately specifying the iron content when modeling planetary interiors. The planetary radius, thermal structure, mineralogy, and overall differentiation state are all closely tied to the distribution and quantity of iron in the system.

3.4 Example 4: Mass variation

Planetary mass (`M`) is the primary input parameter given in Earth masses:

```
interior_structure(M, x_Fe_tot, x_H2O_tot)
```

The mass has a fundamental influence on the resulting interior structure. Unlike compositional parameters such as iron or water content, which primarily affect material distribution and physical properties, mass sets the gravitational context of the entire system, directly influencing pressure, temperature and density. The total mass of the planet is distributed internally as:

$$\text{Mass} = M_{core} + M_{mantle} + M_{water}$$

Which directly relates to the surface gravity:

$$g = \frac{GM}{R^2}$$

Given a fixed iron and water fraction, the absolute masses of the core, mantle, and any water layer scale linearly with total planetary mass. However, the resulting internal structure is governed by non-linear dependencies, as gravitational self-compression becomes increasingly important at higher masses.

Structural implication of mass variation Figure 6 shows how interior profiles vary with planetary mass from 0.1 to 5 Earth masses. Figure 6 can be reproduced by uncommenting the code under the 'Mass variation data' section in the notebook. High-mass planets exhibit stronger gravitational fields, leading to increased pressure and temperature gradients. Density also increases at depth, especially in the core, where compression effects are most crucial.

Benchmarking This modeled response to increasing planetary mass reflects fundamental physical principles governing planetary structure. As such, the results presented in this section serve as a general physical benchmark for interior modeling. Any interior structural model of rocky planets is expected to reproduce these first-order behaviors when mass is systematically increased. Deviations from these trends may point to inconsistencies in equation-of-state implementation, numerical setup, or compositional assumptions. Therefore, this mass variation suite is a useful tool for validating and cross-checking model behavior across different modeling frameworks.

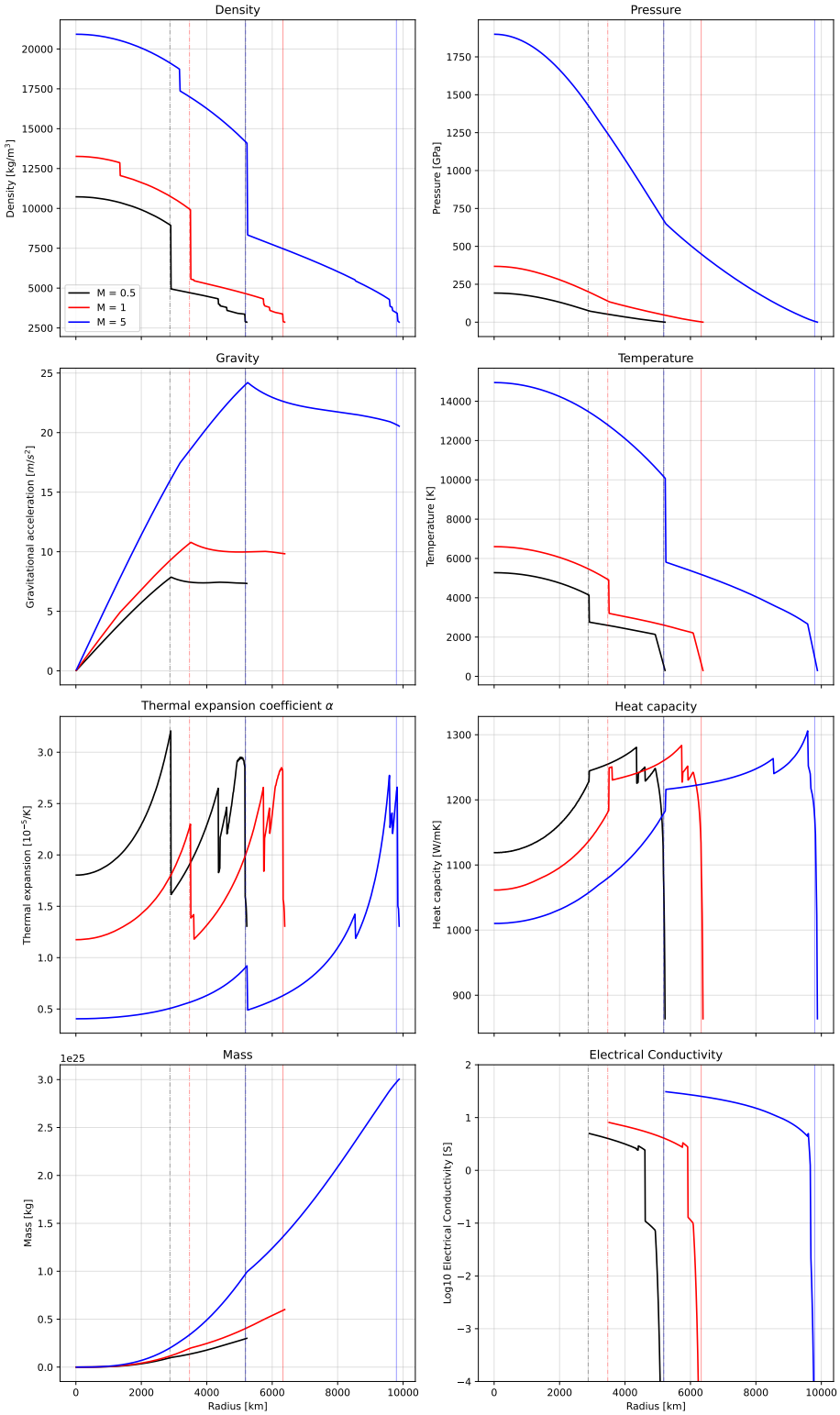

Figure 6: Effect of varying planetary mass on internal structure profiles. The faint dashed lines indicate the core radius, while the faint solid line represents the mantle radius of planets modeled with different planetary masses. All other parameters are held at their default values.

3.5 Application: Mass-Radius plots

The results from the ROWS model can be directly applied to fundamental concepts in planetary science, such as the mass-radius ($M-R$) relation. While it may seem intuitive that a planet's radius should increase proportionally with its mass, this relationship is, in reality, far from linear. If a planet's density profile remains constant, a simple proportional increase could be expected. However, the internal density profile changes significantly with mass. As discussed in Section 3.4, this deviation arises primarily from the increase in gravitational compression at higher planetary masses, which causes interior materials to become increasingly compact. As a result, the rate at which

radius increases with mass, decreases.

This behavior highlights the inherent complexity of the radius-mass relation, which has been the subject of extensive research in planetary science. In general, this relationship can be described by a power-law scaling of the form:

$$\frac{R}{R_\oplus} \propto (\frac{M}{M_\oplus})^\beta$$

where β is the scaling exponent that is composition-dependent. Figure 7 shows how the planetary radius scales with the planetary mass. The obtained data is scaled with the power-law relation. In our modeled case, assuming a FeS-core with 38 wt% iron and no water, we find a best-fit scaling exponent of $\beta \approx 0.271$. This value aligns relatively well with those reported in the literature for low mass exoplanets with an Earth-like composition (1-10 $M_\oplus$): 0.262 [Valencia et al., 2007], 0.274 [Sotin et al., 2007] and 0.267 [Wagner et al., 2011]. The M-R relation is not only of theoretical importance but also plays a crucial role in observational exoplanet science. Since both mass and radius are observable quantities, a well-constrained M-R relation enables inferences about a planet's internal structure and composition.

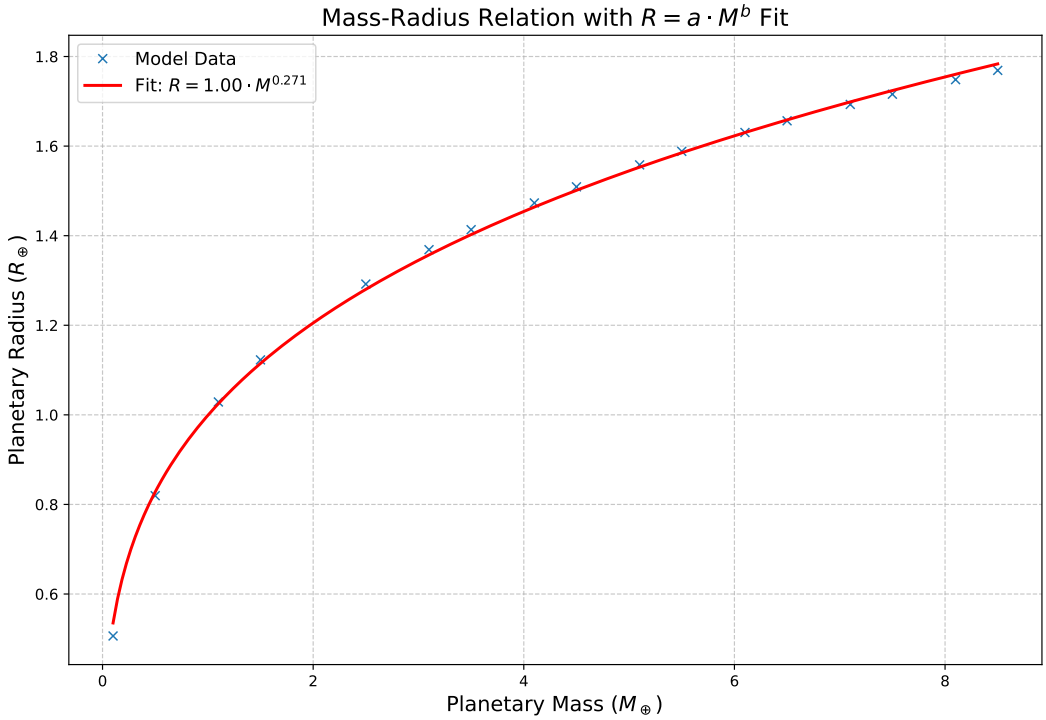

Figure 7: Mass-radius relation derived for different planets with a FeS-core, an iron fraction of 38 wt% and no water. The red line shows a power-law fit with a scaling exponent $\beta \approx 0.271$, which is consistent with literature values.

3.6 Example 5: Core composition

The ROWS Model assumes a core primarily composed of iron, but it also allows for the inclusion of light alloying elements. This is a more realistic representation, as terrestrial planetary cores are generally expected to contain a mixture of iron and lighter elements.

Users can define the alloy composition by selecting a light element to mix with iron (e.g. Fe-FeS), with a specific fraction of lighter elements in the inner and outer core. The fraction of certain light elements in the core are set by `xelem` as an array in the main code, found in the notebook as follows:

```
xelem = np.array([0.0,0.0,0.2,0.0]) # initial core-averaged value
xelem_ic = np.array([0.00,0.00,0.07,0.00]) # fixed inner core value
```

Here `xelem` is set to an array containing the initial average molar fractions of Si, C, S, O in the core. By default, sulfur (`FeS`) is considered and its molar fraction set to 0.2, which is equivalent to a weight fraction of 12 wt-%S. Furthermore, with `xelem_ic` a fixed molar fraction of the lighter elements in the inner core is set. The code includes multiple light-alloy elements that can be utilized. They each correspond to a different iron alloy, which can be found in Table 4.3. This flexibility enables the simulation of more complex core compositions involving multiple light elements alloyed with iron.

The impact of alloying elements is captured through equation of state (EOS) calculations, carried out by the `EOS_functions.py` script with the `EOS_core_mixed` function:

```
cp[i],density[i],alpha[i],KT[i],KS[i],mu[i],V_vec = EOS_core_mixed(pressure[i]/10**9,
    temperature[i],xC=xelemc[1], xSi=xelemc[0], xS=xelemc[2], xO=xelemc[3])
```

This module is used in the main model notebook and computes various interior properties, for the core and rock part of a planet based on the pressure, temperature, and the specified composition. These values directly relate to the resulting core density and the broader interior structure.

By default, the code uses a single alloying element. This is generally sufficient, since the choice of specific light elements tends to have only a modest effect on density, as long as the total fraction of light elements remains the same. This is illustrated in Figure 8, where core densities at 200 GPa and 4000 K are shown for various alloy compositions. The figure highlights the substantial effect that incorporating light elements has on core density: the pure Fe core has a significantly higher density than any other core composition shown. The influence that these light elements have on the core density in turn influences the overall interior structure. Additionally, increasing the abundance of light elements leads to a decrease in core density: the bottom composition which contains an 40% atomic fraction of light elements, results into the lowest core density of all considered compositions. Notably, when comparing the effect of individual light elements, one can observe that the specific choice of light element, whether it be oxygen, sulfur, silicon, or carbon, has a relatively modest influence on the resulting density. Core compositions containing a total of 20% light elements yield similar density values, regardless of the individual light element that is considered.

While modeling different core compositions is possible, current data suggest that the exact identity of light elements in planetary cores is difficult to constrain. The model results are more sensitive to the total abundance of light elements than to their specific types. As such, given the context of this manual, the code defaults to a single alloying element (Fe-FeS), and focuses more on broader structural parameters like total iron and water content.

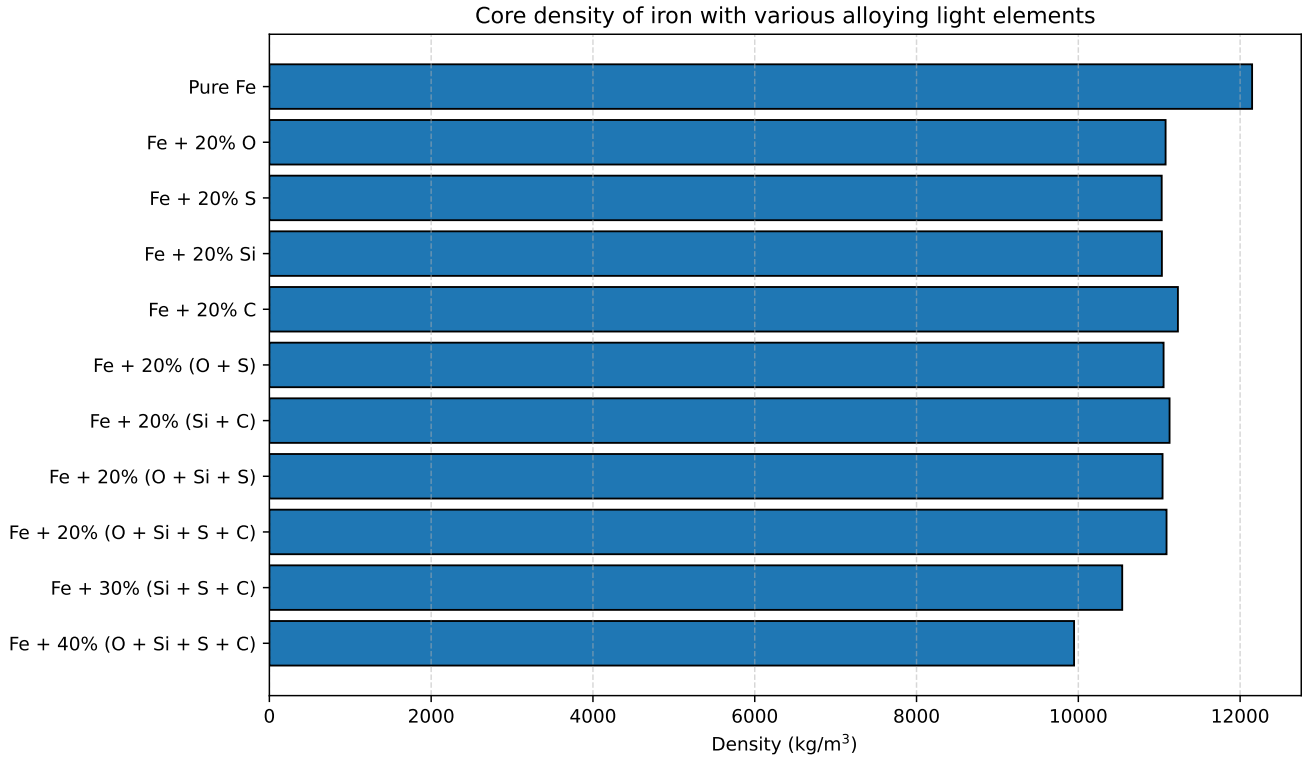

Figure 8: Core density at 200 GPa and 4000 K for iron alloyed with different light elements, computed using the EOS functions. Labels indicate the total atomic fraction of light elements added to Fe. For example, "Fe + 20% O" corresponds to Fe alloyed with 20% oxygen, while "Fe + 20% (O + Si + S + C)" corresponds to a alloy mixture of oxygen, silicon, sulfur and carbon with a combined atomic fraction of 20%. In mixed alloy composition cases, the total light-element fraction is equally distributed over all mixed composition alloy elements. Despite the different compositions, the resulting densities show limited variation, suggesting that the choice of specific light elements has a modest effect on core density at these conditions.

4 Parameter documentation

4.1 Parameters from Interior_Structure.ipynb

The table below shows and explains all the parameters that are found in the code in alphabetical order.

Table 2: Main parameters found in the 1D Interior Structure Code

Variable name	Parameter	Data Type	Description/Notes	Default values	Unit
`Dcr`	Crust thickness	float		50e3	m
`DTcmb`	Temperature jump at core-mantle boundary	float	if set to negative values (e.g. -1): the jump is calculated via melt temperature times -DTcmb	-1.0	K
`Dlid`	Lithosphere thickness	float	The thickness of lithosphere affects the upper-mantle temperature	300e3	m
`G`	Universal Gravitational constant	float		6.67384e-11	$m^3/kg/s^2$
`KS`	Shear modulus	np.ndarray	A measure of the material's resistance to shear deformation at a specific radial point within the interior	Calculated internally	GPa
`KT`	Bulk modulus array	np.ndarray	A measure of the material's resistance to compression at a specific radial point within the interior	Calculated internally	GPa
`M`	Total planetary mass	float	In Earth masses (converted to kg inside function)	1.0 (Input value)	$M_\otimes$
`Mc`	Core mass	float	Based on the planet's iron fraction `x_Fe_tot`	Calculated internally	kg
`Mm`	Mantle mass	float		Calculated internally	kg
`Mw`	Total water mass	float	Based on the planet's water fraction `x_H2O_tot`	Calculated internally	kg
`P_Pa`	Pressure	float	Input argument of temperature melting curve functions		Pa
`P_GPa`	Pressure	float		Calculated internally	GPa
`Psurf`	Atmospheric surface pressure	float		1e5	Pa
`alpha_c` `alpha_m` `alpha_w`	Thermal expansion coefficients	np.darray	Guesses for core, mantle, and water	1e-5, 2.5e-5, 7e-5	1/K
`cp_c` `cp_m` `cp_w`	Heat capacity	float	Guesses for core, mantle, and water	800, 1300, 4200	J/kg K
`density`	Density	np.ndarray	Density at a specific radial point within the interior	Calculated internally	kg/m^3
`dr`	Radial step size	np.ndarray		Calculated internally	m
`ec_model`	Electrical conductivity model	int	1: Xu dry profile, 2: material dependent profile without Fe, 3: as 2 but with Fe-dependency, 4: as 3 but newer parameters (see code for more details)	1	

Variable name	Parameter	Data Type	Description/Notes	Default values	Unit
elcond	Electrical conductivity	np.ndarray	Electrical conductivity at a specific radial point within the interior	Calculated internally	S
elem	Core light element type	str	Specifies which light element to consider in the core (Fe, FeSi, FeC, FeS, FeO)	'FeS'	
fac1	Transition smoothing factor 1	float	Used for calculation of melting temperature curve	10	
fac2	Transition smoothing factor 2	float	Used for calculation of melting temperature curve	0.05	
gravity	Gravitational acceleration	np.ndarray	g at a specific radial point within the interior	Calculated internally	m/s^2
mat	Material	np.ndarray	Material properties index at radial points	Set internally [-1, 7]	
maxIter	Maximum iterations	int	Maximum number of iterations in solver	20	
nr	Radial resolution	int	Number of radial points from center to surface	2000	
p_trans1	Pressure transition 1	float	Pressure boundary between melt regimes 1 and 2	10	GPa
p_trans2	Pressure transition 2	float	Pressure boundary between melt regimes 2 and 3	100	GPa
pressure	Pressure	np.ndarray	Pressure at a specific radial point within the interior	Calculated internally	Pa
radius	Radius	np.ndarray	Radius at a specific radial point within the interior (from center to surface)	Calculated internally	m
rho_c rho_m rho_w	Initial density guesses	float	For core, mantle, and water layers	11000, 4000, 1000	kg/m^3
ratio	Melt fraction ratio	float	Ratio between solidus (0) and liquidus (1), defines melt fraction	0.4	
Rc Rm Rp	Radius of core, mantle shell and planet	float	Requires initial guesses set by initial density and mass guesses	Calculated internally	m
temperature	Temperature	np.ndarray	Temperature at a specific radial point within the interior	Calculated internally	K
Tlid	Lithosphere temperature	float	Temperature at base of lithosphere; if 0, melt temperature at lithosphere depth is used	0.0	K
Tsurf	(Potential) Surface temperature	float		300	K
tol	Convergence tolerance	float	Tolerance for convergence of iterative solver	0.001	
x_Fe	Core iron mass fraction	float	Core mass fraction relative to total planet mass	Calculated internally	
x_Fe_tot	Total iron content	float	Fe content of the planet (converted to fraction inside function)	38 (Input value)	wt%
x_H2O_tot	Total water content	float	H_2O content of the planet (converted to fraction inside function)	0.0 (Input value)	wt%

Variable name	Parameter	Data Type	Description/Notes	Default values	Unit
`xelem`	Molecular fraction of light element in core	float	xelem of 0.2 indicates Fe0.8X0.2, e.g. with 'FeS' this means weight fraction of 12 wt-% S	0.2	
`xelem_ic`	Molecular fraction of light element in inner core	float	Similar to `xelem`, but for inner core	0.07	
`XmFe`	Mantle iron fraction	float	Mantle iron mass fraction relative to mantle mass	Calculated internally	
`X_H2OM`	Water content in mantle	float	Only used for electrical conductivity profile versions 2–4	0	wt%
`X_FeM_mol`	Mantle iron number	float	Ratio Fe-bearing molecules to total Fe- and Mg-bearing molecules in mantle	0.1	

4.2 Minerals

The table below shows all the included minerals, their phase, species and formula in sequential order as defined in `values.py`. Minerals shown in bold represent the default selections used in the code configuration. All mineral data presented in this table and utilized in the code are sourced from Stixrude and Lithgow-Bertelloni [2011].

Phase	Species	Formula
Feldspar (`plg`)	**Anorthite** (`an`)	**Ca[Al2Si2]O8**
Feldspar (`plg`)	Albite (`ab`)	Na[AlSi3]O8
Spinel (`sp`)	Spinel (`sp`)	(Mg3Al)(Al7Mg)Ol6
Spinel (`sp`)	Hercynite (`hc`)	(Fe3Al)(Al7Fe)Ol6
Olivine (`ol`)	**Forsterite** (`fo`)	**Mg2SiO4**
Olivine (`ol`)	**Fayalite** (`fa`)	**Fe2SiO4**
Wadsleyite (`wa`)	**Mg-Wadsleyite** (`mgwa`)	**Mg2SiO4**
Wadsleyite (`wa`)	**Fe-Wadsleyite** (`fewa`)	**Fe2SiO4**
Ringwoodite (`ri`)	**Mg-Ringwoodite** (`mgri`)	**Mg2SiO4**
Ringwoodite (`ri`)	**Fe-Ringwoodite** (`feri`)	**Fe2SiO4**
Orthopyroxene (`opx`)	Enstatite (`en`)	MgMgSi2O6
Orthopyroxene (`opx`)	Ferrosilite (`fs`)	FeFeSi2O6
Orthopyroxene (`opx`)	Mg-Tschermalcs (`mgts`)	MgAl[SiAl]O6
Orthopyroxene (`opx`)	Ortho-Diopside (`odi`)	CaMgSi2O6
Clinopyroxene (`opx`)	**Diopside** (`di`)	**CaMgSi2O6**
Clinopyroxene (`cpx`)	Hedenbergite (`he`)	CaFeSi2O6
Clinopyroxene	Clinoenstatite (`cen`)	MgMgSi2O6
Clinopyroxene	Ca-Tschermaks (`cats`)	CaAl(SiAl)O6
Clinopyroxene	Jadeite (`jd`)	NaAlSi2O6
HP-Clinopyroxene	HP-Clinoenstatite (`hpcen`)	Mg2Si2O6
HP-Clinopyroxene	HP-Clinoferrosilite (`hpcfs`)	Fe2Si2O6
Ca-Perovskite	Ca-Perovskite (`capv`)	CaSiO3
Akimotoite (`ak`)	Mg-Akimotoite (`mgak`)	MgSiO3
Akimotoite	Fe-Akimotoite (`feak`)	FeSiO3
Akimotoite	Corundum (`co`)	AlAlO3
Garnet (`gt.mj`)	Pyrope (`py`)	Mg3AlAlSi3Ol2
Garnet	Almandine (`al`)	Fe3AlAlSi3Ol2
Garnet	Grossular (`gr`)	Ca3AlAlSi3Ol2
Garnet	Mg-Majorite (`mgmj`)	Mg3MgSiSi3Ol2
Garnet	Jd-Majorite (`jdmj`)	(Na2Al)AlSiSi3Ol2
Quartz (`qtz`)	**Quartz** (`qtz`)	**SiO2**
Coesite (`coes`)	Coesite (`coes`)	SiO2
Stishovite (`st`)	Stishovite (`st`)	SiO2
Seifertite (`seif`)	Seifertite (`seif`)	SiO2

Phase	Species	Formula
Perovskite (pv)	**Mg-Perovskite** (mgpv)	**MgSiO3**
Perovskite	**Fe-Perovskite** (fepv)	**FeSiO3**
Perovskite	Rh2O3-II (rh2o3)	AlAlO3
Post-Perovskite	**Mg-Post-Perovskite** (mppv)	**MgSiO3**
Post-Perovskite	**Fe-Post-Perovskite** (fpv)	**FeSiO3**
Post-Perovskite	AI-Post-Perovskite (appv)	AlAlO3
Magnesiowüstite	**Periclase** (pe)	**MgO**
Magnesiowüstite	**Wüstite** (wu)	**FeO**
Ta-Ferrite (cf)	Mg-Ca-Ferrite (mgcf)	MgAlAlO4
Fa-Ferrite	lb-Ta-Ferrite (fecf)	FeAlAlO4
Ca-Ferrite	Na-Ca-Ferrite (nacf)	NaAlSiO4
Kyanite (ky)	Kyanite (ky)	Al2SiO5
Nephclinc (neph)	Nephclinc (neph)	NaAlSiO4

4.3 Iron core phases

The table below shows all the included Iron core phases, in sequential order as defined in `values.py`. The default iron core phase is shown in bold. Data on all phases presented in this table that are utilized in the code are sourced from Bouchet et al. [2013] and Sata et al. [2010].

Species (Code Name)	Formula
Iron (hcp) (fehcp)	Fe (hcp)
Iron Silicide (FeSi)	$Fe_{0.5}Si_{0.5}$
Cementite (Fe3C)	Fe_3C
Wüstite (nonstoichiometric) (FeO)	$Fe_{0.95}O$
Iron Sulfide (VII) (FeS)	**FeS**

*Only valid from 180 GPa on.

References

J. Bouchet, S. Mazevet, G. Morard, F. Guyot, and R. Musella. Ab initio equation of state of iron up to 1500 gpa. *Phys. Rev. B*, 87:094102, Mar 2013. doi: 10.1103/PhysRevB.87.094102. URL https://link.aps.org/doi/10.1103/PhysRevB.87.094102.

A.M. Dziewonski and D.L. Anderson. Preliminary reference earth model. *Physics of the Earth and Planetary Interiors*, 25(4):297–356, 1981. ISSN 0031-9201. doi: https://doi.org/10.1016/0031-9201(81)90046-7. URL https://www.sciencedirect.com/science/article/pii/0031920181900467.

L. Noack, D. Höning, A. Rivoldini, C. Heistracher, N. Zimov, B. Journaux, H. Lammer, T. Van Hoolst, and J.H. Bredehöft. Water-rich planets: How habitable is a water layer deeper than on earth? *Icarus*, 277:215–236, 2016. ISSN 0019-1035. doi: https://doi.org/10.1016/j.icarus.2016.05.009. URL https://www.sciencedirect.com/science/article/pii/S001910351630149X.

N. Sata, K. Hirose, G. Shen, Y. Nakajima, Y. Ohishi, and N. Hirao. Compression of FeSi, Fe_3C, $Fe_{0.95}O$, and FeS under the core pressures and implication for light element in the Earth's core. *Journal of Geophysical Research (Solid Earth)*, 115(B9):B09204, September 2010. doi: 10.1029/2009JB006975.

C. Sotin, O. Grasset, and A. Mocquet. Mass–radius curve for extrasolar earth-like planets and ocean planets. *Icarus*, 191(1):337–351, 2007. ISSN 0019-1035. doi: https://doi.org/10.1016/j.icarus.2007.04.006. URL https://www.sciencedirect.com/science/article/pii/S0019103507001601.

L. Stixrude and C. Lithgow-Bertelloni. Thermodynamics of mantle minerals - ii. phase equilibria. *Geophysical Journal International*, 184(3):1180–1213, 03 2011. ISSN 0956-540X. doi: 10.1111/j.1365-246X.2010.04890.x. URL https://doi.org/10.1111/j.1365-246X.2010.04890.x.

D. Valencia, D.D. Sasselov, and R.J. O'Connell. Detailed models of super-earths: How well can we infer bulk properties? *The Astrophysical Journal*, 665(2):1413, aug 2007. doi: 10.1086/519554. URL https://dx.doi.org/10.1086/519554.

F.W. Wagner, F. Sohl, H. Hussmann, M. Grott, and H. Rauer. Interior structure models of solid exoplanets using material laws in the infinite pressure limit. *Icarus*, 214(2):366–376, 2011. ISSN 0019-1035. doi: https://doi.org/10.1016/j.icarus.2011.05.027. URL https://www.sciencedirect.com/science/article/pii/S0019103511002004.